

# Application of Dynamic Contrast-Enhanced MRI in the Therapeutic Evaluation of the Chinese Medicine Kanglaite in Treating Colorectal Cancer

Yunling Wang,<sup>1</sup> Xiaoqin Li,<sup>2</sup> and Wenxiao Jia<sup>1\*</sup>

<sup>1</sup>Imaging Center, the Second Affiliated Hospital of Xinjiang Medical University, Urumqi, Xinjiang, China

<sup>2</sup>Internal Medicine-Oncology Department, The Third Affiliated Hospital of Xinjiang Medical University, Urumqi, Xinjiang, China

\*Corresponding author: Wenxiao Jia, Imaging Center, the Second Hospital Affiliated Hospital of Xinjiang Medical University, Urumqi 830054, Xinjiang, China. Tel: +86-18599084077, Fax: +86-9913835298, E-mail: 2129867622@qq.com

Received 2017 January 31; Revised 2017 April 22; Accepted 2017 May 08.

## Abstract

**Background:** Magnetic resonance imaging (MRI) can provide a reference for tumor treatment and its quantitative parameters can serve as imaging indicators that reflect tumor angiogenesis and vascularity. Kanglaite (KLT) has therapeutic effects on cancers. In this study, DCE-MRI was used to investigate its application in evaluating KLT anti-colorectal cancer.

**Objectives:** Evaluating the efficacy of Kanglaite (KLT) injection for treatment of colorectal cancer with dynamic contrast-enhanced MRI (DCE-MRI) parameters.

**Methods:** This study was an experimental study. The 20 successfully modeled nude mice were randomly assigned to 2 groups: blank control group (n = 10) and the KLT injection group (n = 10). The research protocol was approved by the ethics committee of the second affiliated hospital of Xinjiang medical university (protocol NO: 20140216-12) in 2015. A subcutaneous xenograft colorectal tumor model was subjected to KLT treatment. DCE-MRI obtain the parameters including Ktrans, Ve, Kep, Vp, immunohistochemical staining measure microvascular density (MVD), levels of vascular endothelial growth factor (VEGF), and proliferating cell nuclear antigen (PCNA).

**Results:** Compared to the blank control, the volume of tumor in the KLT group markedly reduced by 49%. 48 hours after, compared to the blank control, the Ktrans ( $0.028 \pm 0.009$  vs  $0.012 \pm 0.006$ ), Ve ( $0.312 \pm 0.089$  vs  $0.287 \pm 0.037$ ), and Kep values ( $0.321 \pm 0.056$  vs  $0.577 \pm 0.033$ ) decreased in KLT group ( $P < 0.05$ ). In contrast, the Vp value ( $0.094 \pm 0.037$  vs  $0.043 \pm 0.017$ ) was significantly elevated in the KLT group ( $P < 0.05$ ). There is a correlation between Ktrans, Kep and VEGF score, MVD count, and PCNA score.

**Conclusions:** The parameters of DCE-MRI may be used as imaging biomarkers for assessing the status of tumor-bearing vasculatures and provide a basis for evaluating the efficacy of anti-tumor drugs.

**Keywords:** Colorectal Cancer Model, Kanglaite Injection, Dynamic Contrast-Enhanced Magnetic Resonance Imaging

## 1. Background

Numerous studies have shown that the Chinese medicine Kanglaite (KLT) has therapeutic effects on advanced lung, liver, and colorectal cancers, as well as other effects in regulating cell proliferation and the immune system (1). With the gradual integration of modern medicine and traditional Chinese medicine, many traditional Chinese medicines with anti-tumor properties could be developed to benefit cancer patients. Therefore, continuous real-time monitoring of the therapeutic efficacy against tumors is paramount to the development of anti-tumor drugs and the study of their mechanisms. Pathological examination is the current gold standard for diagnosing malignant tumors and has been widely used in the clinical setting. However, the extraction of pathology samples is traumatic for patients, hence, it cannot be repeatedly obtained. Meanwhile, the determination of a

drug's optimal duration of activity, concentration, therapeutic efficacy, and side effects during anti-tumor drug development as well as clinical trials requires effective real-time monitoring of tumor changes, which cannot be done with pathological examination alone (2, 3). Magnetic resonance imaging (MRI) can provide a reference for tumor diagnosis, treatment, and prognosis, and its quantitative parameters can serve as imaging indicators that reflect tumor angiogenesis and vascularity (4, 5). In this study, DCE-MRI was used to investigate its application in evaluating the anti-colorectal cancer efficacy of KLT treatment.

## 2. Methods

### 2.1. Ethics Statement

The research protocol was approved by the ethics committee of the second affiliated hospital of Xinjiang medical university (protocol NO: 20140216-12) in 2015. All the animals were provided appropriate informed consent.

### 2.2. Animals and Groups

This study was an experimental study. BALB/c-nu mice (n = 20) were injected subcutaneously with the human colorectal cancer HT-29 cells. A significant bulge with a volume of 300 mm<sup>3</sup> was observed at the graft site after 15 days. The tumor had a hard texture, low flexibility, and was closely bound to the skin. The 20 successfully modeled nude mice were randomly assigned to 2 groups: 10 mice in the blank control group and the other 10 in the KLT injection group. Animals were provided by the SPF animal laboratory of the Shanghai institutes for biological sciences. All animals were healthy and handled with standard conditions of temperature, humidity, 12 hours light/dark cycle, free access to food as well as water, and without any intended stress stimuli. All experimental procedures were approved by the animal ethics committee of the second affiliated hospital of Xinjiang medical university. The study was performed during February 2014 to February 2016 in Urumqi city, Xinjiang, China.

Sample size formula:  $N = 2 \times [(1.96 + 1.282) \times S/X]^2$ . S: standard deviation; X: mean difference

### 2.3. MRI Detection Time and Equipment

MRI scans were performed 15 days after modeling with the 3.0 T Tim Avanto MRI scanner (Siemens, Germany) and the 25 mm RF coil dedicated for experimental animal use (developed by Shanghai Chenguang medical technologies Co, LTD.; patent #: ZL201020236347.3). The MRI scan sequences and parameters are as follows: T1WI-TSE sequence: TR = 280, TE = 18, slice thickness = 2 mm, inter-slice distance = 0.0 mm, slices = 10, FOV = 70, number of signal averages (NSA) = 3, and matrix = 256 × 256. T2WI-TSE sequence: TR = 3000, TE = 82, slice thickness = 2 mm, inter-slice distance = 0.0 mm, slices = 10, FOV = 70, NSA = 3, and matrix = 512 × 512. DCE scan parameters: TR = 9.0, TE = 1.28, slice thickness = 2 mm, inter-slice distance = 0.4 mm, slices = 16 - 20, FOV = 62, NSA = 1, matrix = 128 × 94, arterial phase numbers = 100, and 15 dynamic time phases in baseline scans. Gadopentetate dimeglumine-diethylenetriaminepentaacetic acid (Gd-DTPA) was used as the contrast agent for MRI with a concentration of 0.06 mmol/mL, injected into the tail vein at a speed of 0.30 mmol/kg.

### 2.4. Immunohistochemical Staining

#### 2.4.1. Determination of Microvascular Density

CD34 antibody (purchased from Xinjiang Urumqi Baoxin biological reagent Co. Ltd.) was used for staining. The criterion was the internationally used Weidner method with some modifications: first scan the entire slide at lower power (× 100), identify the “hot spot” of highest microvessel density, and then observe and count the microvessels at higher power (× 200). Any individual cell or cell aggregate that was stained brown by the antibody, regardless of whether they formed the lumen of a vessel and as long as they showed a distinct separation from the surrounding microvessels, tumor, and connective tissues, was considered to be 1 countable vessel. Microvessels in hardened areas of the tumor and at the boundary between the tumor and soft tissue were not counted. Vessels with a thick, smooth muscle or a lumen cross-sectional area larger than the diameter of 8 red blood cells were also excluded. The number of microvessels from 5 microscopic fields was recorded according to this standard, and the average was the MVD count.

#### 2.4.2. Detection of Vascular Endothelial Growth Factor

VEGF monoclonal antibody (purchased from Xinjiang Urumqi Baoxin biological reagent Co. Ltd.) was used for staining. Scoring criteria was based on both the staining intensity and the percentage of VEGF-positive cells. Given that non-specific staining was excluded, scoring of staining intensity was performed first: 0 was colorless, 1 point for light yellow, 2 points for brownish-yellow, and 3 points for brown. Then scoring was done for the percentage of positive cells: 0 points for negative, 1 point for < 10% positive, 2 points for 11% - 50% positive, 3 points for 51% - 75% positive, and 4 points for > 75% positive. Product of staining intensity and percentage of positive cells > 3 was considered to be positive immunoreactivity. The product scores were ranked into 4 categories: - (0, 1, 2 points), + (3 - 5 points), ++ (6 - 8 points), +++ (9 - 12 points).

### 2.5. Statistical Methods

All data were recorded into the database in tabular form and were expressed as mean ± SD. Measurement data were compared between the 2 groups using independent sample t-test, the comparison between the 3 groups were analyzed by ANOVA or non-parametric tests depending on the homogeneity of variance. Count data were analyzed by the Chi-square test. The diagnostic test and correlation analysis were used to analyze the correspondence between imaging indicators at different stages of pathology and the pathological results. Measurement data were analyzed by multiple linear regression and ranked data were analyzed

by logistic regression. All data were analyzed using the SPSS 21.0 software and  $P < 0.05$  was considered to be statistically significant.

### 3. Results

#### 3.1. KLT Significantly Inhibited the Growth of the Subcutaneous Xenograft Tumor in Nude Mice

15 days following subcutaneous inoculation of human colorectal cancer HT-29 cells in nude mice, a significant bulge of volume  $300 \text{ mm}^3$  was observed at the site of inoculation. The tumor had a hard texture, low flexibility, and was closely bound to the skin. At 48 hours after KLT injection, the volume of the subcutaneous xenograft tumor significantly decreased by 49% compared to the blank control (Figure 1).

#### 3.2. DCE-MRI Results of KLT Group and Control Group

Compared with the blank control group, Ktrans and Kep value decreased significantly in the Kanglaite group, the difference was statistically significant ( $P < 0.05$ ); the Ve value increased slightly, there was no statistically significant difference ( $P > 0.05$ ); Vp increased significantly in the injection group, the difference was statistically significant ( $P < 0.05$ ). See Table 1 and Figures 2 and 3.

#### 3.3. Pathological Immunohistochemical Staining

The MVD counts and CD34-positive neovasculatures significantly decreased in the KLT group, and neovascularization was only found at the edge of the tumor. The ratio of PCNA-positive cells markedly decreased in the KLT group (Table 2 and Figure 4).

#### 3.4. Correlation Analysis of Immunohistochemical Staining Results and DCE-MRI Parameters After KLT Treatment

DCE-MRI Ktrans value, Kep and VEGF score, MVD count and PCNA score have positive correlation, the difference was statistically significant ( $P < 0.05$ ). A significant linear correlation ( $P > 0.05$ ) does not exist in the results of Ve and Vp as well as immunohistochemical. See Table 3.

### 4. Discussion

Although surgery is the preferred treatment for cancer, some patients with advanced tumors are unable to withstand surgical trauma and can only turn to other treatments such as chemotherapy or radiotherapy. Chemotherapy refers to the use of chemical drugs to inhibit tumor cell proliferation, invasion, and metastasis (6). Chemotherapy damages normal cells greatly while also killing tumor

cells, resulting in side effects and adverse reactions. Traditional Chinese medicine is a unique medical practice of China, and it has made tremendous contributions to the world's healthcare and the comprehensive treatment of tumors (7, 8). Studies have shown that KLT has certain therapeutic effects on advanced lung, liver, and colorectal cancers, and it can also regulate the immune system and enhance the tumor-killing effects of chemotherapy (9, 10).

Due to the fact that DCE-MRI can show the blood perfusion in tumor microcirculation, the technique has been widely used in clinical therapeutic efficacy evaluations of chemotherapy and targeted therapies for treating tumors (11, 12). In this study, DCE-MRI was used as an assessment of the anti-tumor efficacy of KLT injection for the purpose of evaluating the therapeutic efficacy of an anti-tumor Chinese medicine. Results indicated that at 48 hours post-KLT treatment, the DCE-MRI parameters that showed relatively strong positive correlations with VEGF score and MVD counts included the Ktrans, MSI, and Kep. These indicators showing high correlations were statistically significant, indicating that KLT can effectively inhibit the growth of tumors by inhibiting tumor microcirculation. Meanwhile, Ktrans, Kep, and PCNA score also showed good positive correlations with each other, which could be due to two reasons. First, KLT treatment induced the reduction of blood perfusion, leading to lower nutrient and oxygen supplies for the tumor, which ultimately resulted in a decrease in the proliferation rate of tumor cells as indicated by the proportion of PCNA-positive cells. Second, our in vitro results demonstrated that KLT treatment could inhibit the proliferation and promote the apoptosis of colorectal cancer cells, which directly resulted in a reduced ratio of PCNA-positive cells. Many studies have confirmed that Ktrans and Kep are very effective parameters for evaluating the efficacy of anti-tumor angiogenesis drugs such as bevacizumab (13, 14). Results from this study have added additional support for this conclusion as we demonstrated that DCE-MRI, especially the parameters Ktrans and Kep, have great potential for assessing and predicting the therapeutic efficacy of anti-tumor Chinese medicines.

KLT can significantly inhibit the growth of subcutaneously grafted tumors in nude mice through the possible mechanisms of promoting apoptosis and inhibiting proliferation in the tumor. However, further studies are required to elucidate which of the 2 mechanisms plays the dominant role in the anti-tumor effect of KLT. It was demonstrated in this study that KLT injection therapy can inhibit the angiogenesis and proliferative activity of tumor cells, with a relatively good correlation with pathological test results. In particular, parameters such as Ktrans and Kep have satisfactory clinical and research value as they can serve as effective indicators for assessing the efficacy of

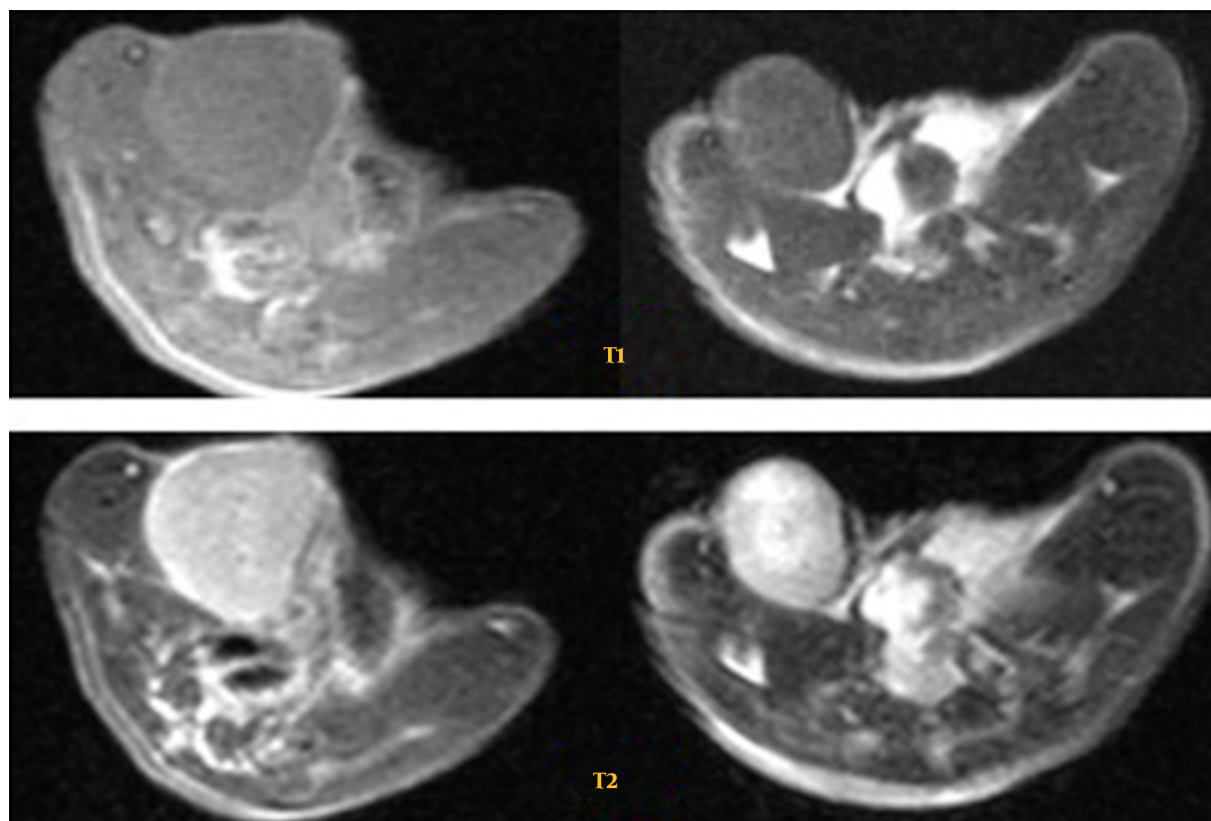


**Figure 1.** The Volume of Xenograft Tumor Following Intraperitoneal Injection of KLT (left) Significantly Decreased Compared to the Control (right).

**Table 1.** Statistics of DCE-MRI Measurements in Each Group After Treatment<sup>a</sup>

| Treatment      | Cases | $k^{trans}$       | Ve                | Vp                | Ke <sub>p</sub>   |
|----------------|-------|-------------------|-------------------|-------------------|-------------------|
| Control        | 10    | $0.028 \pm 0.009$ | $0.312 \pm 0.089$ | $0.321 \pm 0.056$ | $0.094 \pm 0.037$ |
| KLT            | 10    | $0.012 \pm 0.006$ | $0.287 \pm 0.037$ | $0.377 \pm 0.033$ | $0.043 \pm 0.017$ |
| <b>F value</b> |       | 34.450            | 1.659             | 7.365             | 29.448            |
| <b>P value</b> |       | < 0.001           | 0.196             | 0.001             | < 0.001           |

<sup>a</sup>Compared to the blank control, the  $k^{trans}$  and  $Ke_p$  values in the KLT group were significantly reduced ( $P < 0.05$ ); Ve value slightly increased, but was not statistically significant ( $P > 0.05$ ); Vp markedly increased in the KLT group ( $P < 0.05$ ).

**Table 2.** Statistical Analysis of IHC Staining Results of Each Group After Treatment<sup>a</sup>

| Treatment      | Case | MVD Counts        | VEGF Score        | Percentage of PCNA-Positive Cells (%) |
|----------------|------|-------------------|-------------------|---------------------------------------|
| Control        | 10   | $11.7 \pm 2.52$   | $4.43 \pm 1.07$   | $91.23 \pm 8.23$                      |
| KLT            | 10   | $4.96 \pm 1.96^b$ | $2.23 \pm 1.03^b$ | $49.62 \pm 4.36^b$                    |
| <b>F value</b> |      | 4.96              | 6.12              | 10.29                                 |
| <b>P value</b> |      | 0.023             | 0.009             | < 0.001                               |

<sup>a</sup>The MVD counts, VEGF score, and percentage of PCNA-positive cells significantly decreased in the KLT group ( $P < 0.05$ ).

<sup>b</sup> $P < 0.05$ .

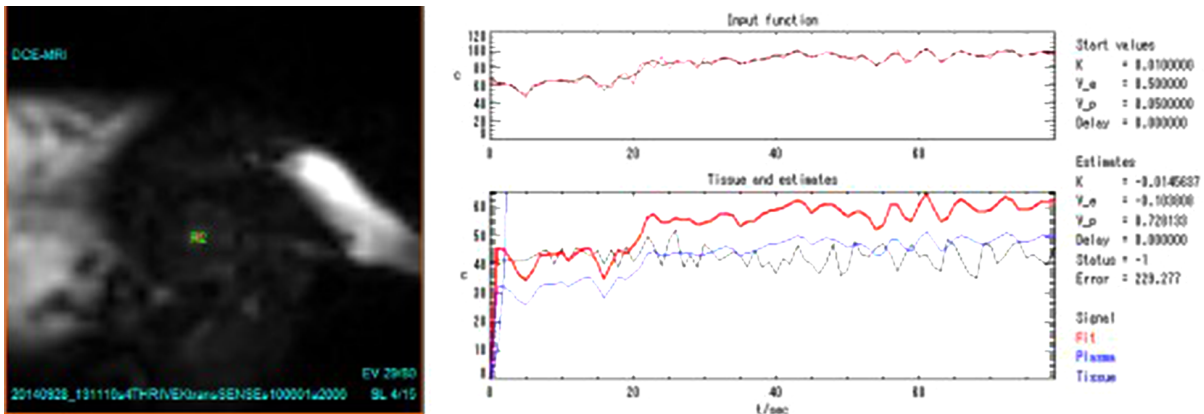


Figure 2. Measurement of Quantitative DCE-MRI Parameters in Blank Control Group

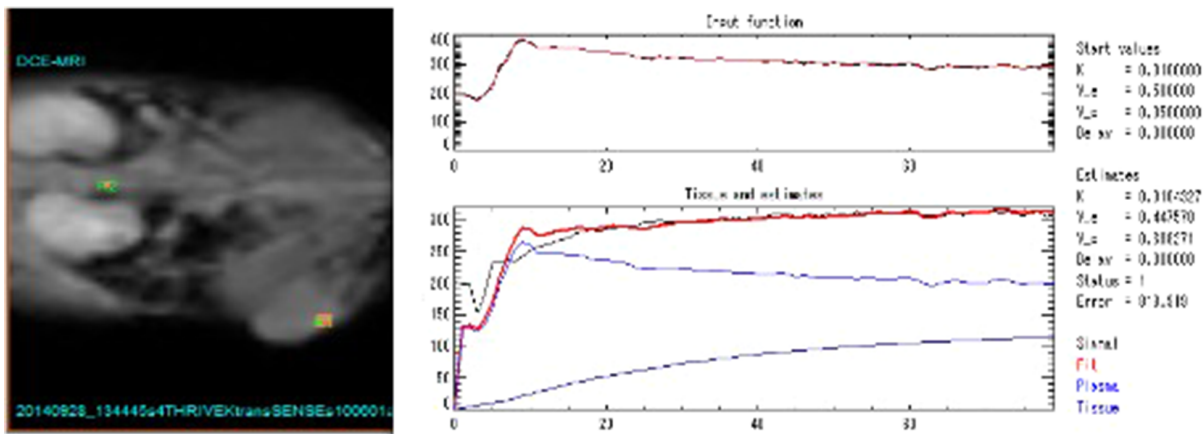


Figure 3. Measurement of Quantitative DCE-MRI Parameters in KLT Group

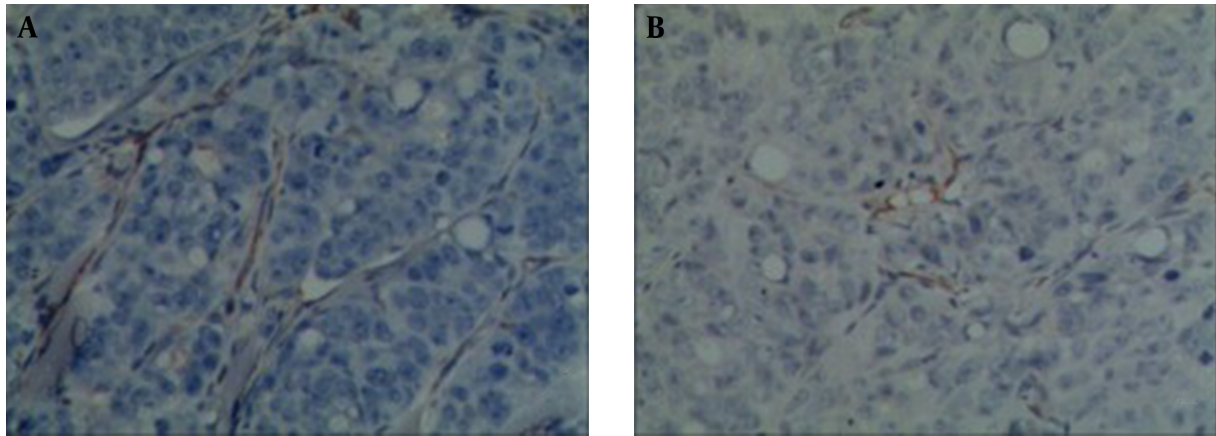
Table 3. Correlation Analysis of Immunohistochemical Staining Results and Various DCE-MRI Parameters<sup>a</sup>

| IHC        |         | $k^{trans}$        | Ve    | Vp    | Kep                |
|------------|---------|--------------------|-------|-------|--------------------|
| MVD counts | r value | 0.879 <sup>b</sup> | 0.203 | 0.251 | 0.596 <sup>b</sup> |
|            | P value | < 0.001            | 0.175 | 0.163 | < 0.001            |
| VEGF score | r value | 0.796 <sup>b</sup> | 0.163 | 0.212 | 0.586 <sup>b</sup> |
|            | P value | < 0.001            | 0.302 | 0.201 | < 0.001            |
| PCNA score | r value | 0.661 <sup>b</sup> | 0.176 | 0.296 | 0.496 <sup>b</sup> |
|            | P value | < 0.001            | 0.323 | 0.151 | 0.001              |

<sup>a</sup>  $k^{trans}$  and  $K_{ep}$  values of DCE-MRI have a relatively strong positive correlation with VEGF score, MVD counts, and PCNA score ( $P < 0.05$ );  $V_e$  and  $V_p$  showed no significant linear correlation with the IHC results ( $P > 0.05$ ).

<sup>b</sup> Indicates  $P < 0.05$ .

anti-tumor Chinese medicines.

**Figure 4.** CD34 Immunostaining of Xenograft Tumor Tissue

A, blank control group: positive staining of vascular endothelial cells can be found in tumor stroma. MVD indicates the high density area (IHC  $\times 200 \times$ ) in the control group; B, KLT group: vascular endothelial cells can only be found scattered at the margins of the tumor as shown by the yellowish-brown staining. MVD indicates the low density area (IHC  $\times 200 \times$ ) after KLT treatment.

#### 4.1. Weak and Strong Points of Study

**Strong points:** This study evaluated treatment of KLT injection for colorectal cancer by DCE-MRI parameters combined with the immunohistochemical staining method.

**Weak points:** The study did not establish a positive control group.

#### 4.2. The Novelty of Study

DCE-MRI evaluation of traditional Chinese medicine Kanglaite Injection for treating colorectal cancer by quantifying tumor angiogenesis and tumor vascular imaging.

#### Acknowledgments

This work was supported by grant from the national natural science foundation (31360213).

#### Footnote

**Financial Disclosure:** None.

#### References

- Xue NZ, Fang RM, Lin LZ. Application of Response Evaluation Criteria of Traditional Chinese Medicine for Solid Tumor in advanced non-small cell lung cancer. *Chin J Integr Med.* 2014;**20**(12):910-6. doi: [10.1007/s11655-014-2022-0](https://doi.org/10.1007/s11655-014-2022-0). [PubMed: [25428339](https://pubmed.ncbi.nlm.nih.gov/25428339/)].
- Chen YT. Detection of cancer/testis antigens as a diagnostic tool in routine pathology practice. *Oncoimmunology.* 2014;**3**:28132. doi: [10.4161/onci.28132](https://doi.org/10.4161/onci.28132). [PubMed: [25340008](https://pubmed.ncbi.nlm.nih.gov/25340008/)].
- Beugeling M, Ewing-Graham PC, Mzallassi Z, van Doorn HC. Pathology slide review in vulvar cancer does not change patient management. *ISRN Surg.* 2014;**2014**:385386. doi: [10.1155/2014/385386](https://doi.org/10.1155/2014/385386). [PubMed: [25006513](https://pubmed.ncbi.nlm.nih.gov/25006513/)].
- Vinh NQ, Naka S, Cabral H, Murayama H, Kaida S, Kataoka K, et al. MRI-detectable polymeric micelles incorporating platinum anticancer drugs enhance survival in an advanced hepatocellular carcinoma model. *Int J Nanomedicine.* 2015;**10**:4137-47. doi: [10.2147/IJN.S81339](https://doi.org/10.2147/IJN.S81339). [PubMed: [26203241](https://pubmed.ncbi.nlm.nih.gov/26203241/)].
- Singh A, Dilnawaz F, Mewar S, Sharma U, Jagannathan NR, Sahoo SK. Composite polymeric magnetic nanoparticles for co-delivery of hydrophobic and hydrophilic anticancer drugs and MRI imaging for cancer therapy. *ACS Appl Mater Interfaces.* 2011;**3**(3):842-56. doi: [10.1021/am101196v](https://doi.org/10.1021/am101196v). [PubMed: [21370886](https://pubmed.ncbi.nlm.nih.gov/21370886/)].
- Kamat N, Khidhir MA, Hussain S, Alashari MM, Rannug U. Chemotherapy induced microsatellite instability and loss of heterozygosity in chromosomes 2, 5, 10, and 17 in solid tumor patients. *Cancer Cell Int.* 2014;**14**(1):118. doi: [10.1186/s12935-014-0118-4](https://doi.org/10.1186/s12935-014-0118-4). [PubMed: [25493073](https://pubmed.ncbi.nlm.nih.gov/25493073/)].
- Wang YJ, Li Q, Li YJ, Yang Q, Chen Y, Weng XG, et al. [Current status of traditional Chinese medicine on reversing tumor multi-drug resistance]. *Zhongguo Zhong Yao Za Zhi.* 2014;**39**(24):4693-8. [PubMed: [25898563](https://pubmed.ncbi.nlm.nih.gov/25898563/)].
- Li F, Zhang W. Role of traditional Chinese medicine and its chemical components in anti-tumor metastasis. *J Cancer Res Ther.* 2014;**10 Suppl 1**:20-6. doi: [10.4103/0973-1482.139748](https://doi.org/10.4103/0973-1482.139748). [PubMed: [25207886](https://pubmed.ncbi.nlm.nih.gov/25207886/)].
- Liu X, Yang Q, Xi Y, Yu K, Wang W, Zhao X, et al. Kanglaite injection combined with chemotherapy versus chemotherapy alone in the treatment of advanced non-small cell lung carcinoma. *J Cancer Res Ther.* 2014;**10 Suppl 1**:46-51. doi: [10.4103/0973-1482.139758](https://doi.org/10.4103/0973-1482.139758). [PubMed: [25207891](https://pubmed.ncbi.nlm.nih.gov/25207891/)].
- Huang X, Qin J, Lu S. Kanglaite stimulates anticancer immune responses and inhibits HepG2 cell transplantation-induced tumor growth. *Mol Med Rep.* 2014;**10**(4):2153-9. doi: [10.3892/mmr.2014.2479](https://doi.org/10.3892/mmr.2014.2479). [PubMed: [25119060](https://pubmed.ncbi.nlm.nih.gov/25119060/)].
- Stange R, Sahin H, Wieskotter B, Persigehl T, Ring J, Bremer C, et al. In vivo monitoring of angiogenesis during tendon repair: a novel MRI-based technique in a rat patellar tendon model. *Knee Surg Sports Traumatol Arthrosc.* 2015;**23**(8):2433-9. doi: [10.1007/s00167-014-2897-5](https://doi.org/10.1007/s00167-014-2897-5). [PubMed: [24519623](https://pubmed.ncbi.nlm.nih.gov/24519623/)].

12. Huang SY, Chen BB, Lu HY, Lin HH, Wei SY, Hsu SC, et al. Correlation among DCE-MRI measurements of bone marrow angiogenesis, microvessel density, and extramedullary disease in patients with multiple myeloma. *Am J Hematol*. 2012;**87**(8):837-9. doi: [10.1002/ajh.23256](https://doi.org/10.1002/ajh.23256). [PubMed: [22718413](https://pubmed.ncbi.nlm.nih.gov/22718413/)].
13. Qiu LH, Zhang JW, Li SP, Xie C, Yao ZW, Feng XY. Molecular imaging of angiogenesis to delineate the tumor margins in glioma rat model with endoglin-targeted paramagnetic liposomes using 3T MRI. *J Magn Reson Imaging*. 2015;**41**(4):1056-64. doi: [10.1002/jmri.24628](https://doi.org/10.1002/jmri.24628). [PubMed: [24677456](https://pubmed.ncbi.nlm.nih.gov/24677456/)].
14. Conway AE, Reddick WE, Li Y, Yuan Y, Glass JO, Baker JN, et al. "Occult" post-contrast signal enhancement in pediatric diffuse intrinsic pontine glioma is the MRI marker of angiogenesis? *Neuroradiology*. 2014;**56**(5):405-12. doi: [10.1007/s00234-014-1348-9](https://doi.org/10.1007/s00234-014-1348-9). [PubMed: [24626721](https://pubmed.ncbi.nlm.nih.gov/24626721/)].